THE JOURNAL OF BIOLOGICAL CHEMISTRY VOL. 291, NO. 36, pp. 19018–19030, September 2, 2016
© 2016 by The American Society for Biochemistry and Molecular Biology, Inc. Published in the U.S.A.

EspR-dependent ESAT-6 Protein Secretion of *Mycobacterium tuberculosis* Requires the Presence of Virulence Regulator PhoP*[S]

Received for publication, July 1, 2016, and in revised form, July 20, 2016 Published, JBC Papers in Press, July 21, 2016, DOI 10.1074/jbc.M116.746289

Vijjamarri Anil Kumar[1,2], **Rajni Goyal**[2,3], **Roohi Bansal**[4], **Nisha Singh**[1], **Ritesh Rajesh Sevalkar**[1], **Ashwani Kumar**, **and Dibyendu Sarkar**[5]

From the Council of Scientific and Industrial Research-Institute of Microbial Technology, Sector 39 A, Chandigarh 160036, India

Attenuation of *Mycobacterium bovis* BCG strain is related to the loss of the RD1-encoded ESX-1 secretion system. The ESX-1 system secretes virulence factor ESAT-6 that plays a critical role in modulation of the host immune system, which is essential for establishment of a productive infection. Previous studies suggest that among the reasons for attenuation of *Mycobacterium tuberculosis* H37Ra is a mutation in the *phoP* gene that interferes with the ESX-1 secretion system and inhibits secretion of ESAT-6. Here, we identify a totally different and distinct regulatory mechanism involving PhoP and transcription regulator EspR on transcriptional control of the *espACD* operon, which is required for ESX-1-dependent ESAT-6 secretion. Although both of these regulators are capable of influencing *espACD* expression, we show that activation of *espACD* requires direct recruitment of both PhoP and EspR at the *espACD* promoter. The most fundamental insights are derived from the inhibition of EspR binding at the *espACD* regulatory region of the *phoP* mutant strain because of PhoP-EspR protein-protein interactions. Based on these results, a model is proposed suggesting how PhoP and EspR protein-protein interactions contribute to activation of *espACD* expression and, in turn, control ESAT-6 secretion, an essential pathogenic determinant of *M. tuberculosis*. Together, these results have significant implications on the mechanism of virulence regulation of *M. tuberculosis*.

Mycobacterium tuberculosis uses the ESX-1 secretion system to transport virulence factors in host cells (1–5). ESX-1 secretion system is encoded by the genes of the *esx-1* locus, which is highly conserved in members of the *M. tuberculosis* complex and in other pathogenic mycobacteria (5–9). The best known ESX-1 substrates, the secreted proteins EsxA (ESAT-6) and EsxB (CFP10), have been implicated in the majority of the ESX-1-dependent modulations of host cell defense (10–19) and therefore are considered to be essential for virulence (12–14). Consistently, deletion of the *esx-1* locus abrogates ESX-1-dependent secretion and strongly attenuates *M. tuberculosis* (15, 20). Notably, the genes encoding *esx-1*, located within the *M. tuberculosis* RD1 locus, are absent in the attenuated *Mycobacterium bovis* BCG and the potential vaccine strain *Mycobacterium microti* (15, 17). However, a chromosomally unlinked non-RD1 locus (Rv3616c-Rv3615c-Rv3614c, also designated as *espA*, *espC*, and *espD*) is essential for ESX-1 function (13, 21). In fact, EspA and EspC proteins themselves are substrates of the ESX-1 secretion system, thus constituting mutually dependent secretion of substrates, a notable feature of this secretion system. More recently, EspA of the tubercle bacilli has been implicated as a critical mediator of bacterial cell wall integrity and ESX-1-dependent virulence regulation (22).

ESX-1 represents the first and the most characterized member of the ESX secretion family. Although intracellular concentrations of ESAT-6 are similar in both virulent *M. tuberculosis* H37Rv and the attenuated strain of *M. tuberculosis* H37Ra, the H37Ra remains defective for ESAT-6 secretion as are the *phoP* mutants of *M. tuberculosis* H37Rv (13). It was shown that a single nucleotide polymorphism within the PhoP C-terminal domain of *M. tuberculosis* H37Ra accounts for its defect in ESAT-6 secretion (23). Remarkably, the introduction of H37Rv.PhoP into H37Ra restored ESAT-6 secretion, establishing a clear link between PhoP and secretion of ESAT-6/CFP-10 (24). Additionally, *espB* of the extended RD1 locus, *espR* (25), and the *espACD* operon (Rv3616c-Rv3615c-Rv3614c) of the non-RD1 locus, which is essential for ESAT-6 secretion (21), were shown to be down-regulated by *M. tuberculosis* PhoP (24, 26, 27). Given the relationship that exists between EspA expression with ESAT-6 secretion (13) on the one hand and between the expression of *espACD* and the response regulator PhoP (24, 26, 27) on the other hand, we sought to investigate the role of PhoP in ESX-1-dependent ESAT-6 secretion.

At the level of regulation, precise control of the *espACD* operon is rather complex and multifactorial. Consistent with this, six different DNA binding regulators, namely cyclic AMP receptor protein (CRP)[6] (28), response regulator PhoP of the

* This work was supported in part by the Supra Institutional Project on Infectious Disease from the Council of Scientific and Industrial Research, research grants (to D. S.) from the Department of Science and Technology, and grants from the Department of Biotechnology, Government of India. The authors declare that they have no conflicts of interest with the contents of this article.
[S] This article contains supplemental Tables S1 and S2 and Figs. S1–S6.
[1] Supported by fellowships from the CSIR.
[2] Both authors contributed equally to this work.
[3] Supported by the Indian Council of Medical Research. Present address: Dept. of Microbiology and Molecular Genetics, Michigan State University, East Lansing, MI 48824.
[4] Supported by the University Grants Commission, Government of India.
[5] Recipient of funding from the National Bioscience Award for career development from the Department of Biotechnology, Government of India. To whom correspondence should be addressed. Tel.: 91-172-6665291; Fax: 91-172-2690585; E-mail: dibyendu@imtech.res.in.

[6] The abbreviations used are: CRP, cyclic AMP receptor protein; DC, dendritic cell; IP, immunoprecipitation; qPCR, quantitative PCR; M-PFC, mycobacterial protein fragment complementation.

phoP-phoR two-component system (23, 27), EspR protein (ESX-1 secreted protein regulator) (29), nucleoid-associated protein Lsr2 (30), response regulator MprA (31), and WhiB6 (32), are known to influence *espACD* expression. Two recent reviews implicate PhoP and EspR in regulating the *espACD* operon highlighting the importance of the PhoP-EspR-*espACD* regulatory circuit in the control of ESAT-6 secretion (33, 34). Also, MprA has been shown to function as a repressor of *espA* expression with MprA boxes being identified close to EspR-binding sites (31). However, thus far, the mechanism of regulation of *espACD* expression remains largely unknown. Regulation of the *espACD* locus by PhoP was originally shown by using a *phoP* disruption mutant (27) and by using *M. tuberculosis* H37Ra and a *phoP*-complemented H37Ra strain (23). These findings were extended to several *M. tuberculosis* strains to trace how discrete mutations in the *phoPR* virulence regulator could inactivate certain virulence factors and how different compensatory mutations could allow recovery of protein and lipid production (35, 36). To examine whether altered expression of *espACD* in a *phoP* mutant of *M. tuberculosis* compensates for ESAT-6 secretion, Gonzalo-Asensio *et al.* (36) were able to restore ESAT-6 secretion by complementing Δ*phoPR* with the *M. bovis espACD* region. Notably, *espACD-TB* carrying the corresponding region of the *M. tuberculosis espACD* allele could not restore ESAT-6 secretion (36). Importantly, *espACD-TB* used in these experiments, lacking the RD8 region, discussed below, contained the only reported PhoP-binding site (37) but lacked the major EspR-binding site (38). More recently, it has been shown that although PhoP is able to bind to the *espR* promoter, it fails to bind to the *espACD* promoter on its own (39). However, EspR has been shown to directly bind and activate the *espACD* operon involving long range interactions between EspR and the *espA* regulatory region (38, 40). In addition, EspR expression was shown to be under direct control of PhoP (25, 41) with a consensus PhoP-binding motif within the *espR* promoter (37, 42). However, the role of PhoP in ESX-1-dependent secretion and virulence has remained unclear and puzzling.

In this study, we document a novel mechanism of PhoP in ESX-1-dependent ESAT-6 secretion. Whereas failure to activate *espACD* synthesis by the *phoP* mutant accounts for the absence of ESAT-6 secretion, we provide evidence showing that synergistic activation of the *espACD* operon requires the simultaneous presence of both PhoP and EspR at the *espACD* promoter. Strikingly, results reported in this study account for explanations of how EspR-dependent activation of the *espACD* locus (29) is linked to positive regulation of the same operon by PhoP (23). Together, these results underscore a crucial role of PhoP in ESX-1 secretion machinery via a complex mode of action and elaborate on the mechanism of transcription regulation of *espACD* by the functional cooperation of the one-component and two-component regulator.

Results

PhoP-dependent espACD Activation Regulates ESX-1-dependent ESAT-6 Secretion—We wished to investigate which of the ESX-1 system-associated genes are regulated by PhoP. To this effect, we compared the expression of *espA*, *espB*, and *espR* in WT, Δ*phoP*, and Δ*phoP* complemented strain by RT-PCR using PAGE-purified gene-specific primers (supplemental Table S2). Although *espB* expression was comparable (1 ± 0.05-fold) in WT and Δ*phoP*, the transcripts of *espR*, and *espA* were detectable at 2.3 ± 0.2- and 6 ± 0.4-fold lower levels in the mutant compared with the WT strain (Fig. 1*A*). Consistent with the RT-PCR results, EspA expression was >10-fold down-regulated in the mutant strain compared with WT *M. tuberculosis* (Fig. 1*B*). However, the EspR protein level displayed almost comparable expression in the WT and the Δ*phoP* mutant. Note that *espC* and *espD* genes of the *espACD* operon (43) showed 5.6 ± 0.8- and 5.8 ± 0.4-fold lower expression levels, respectively, in the Δ*phoP* mutant relative to WT *M. tuberculosis* (supplemental Fig. S1).

Next, we wanted to examine the effect of expression of *espACD*, *espB*, or *espR* in Δ*phoP* to assess their influence on ESAT-6 secretion. Thus, mutant strains ectopically expressing the indicated genes (Table 1) were grown as described under "Experimental Procedures," and culture filtrates as well as cell lysates were collected. As expected, Δ*phoP* failed to show ESAT-6 secretion. However, Δ*phoP* complemented with *phoP* could fully restore antigen secretion (Fig. 1*C*). Importantly, Δ*phoP* expressing *espR* and *espB* failed to show ESAT-6 secretion. In sharp contrast, Δ*phoP* expressing *espACD* locus restored ESAT-6 secretion at the level of WT *M. tuberculosis* H37Rv. To verify levels of *espACD* expression in mutant strains, we performed RT-PCR analysis (Fig. 1*D*). Our results confirm that complementation with *phoP* could restore *espACD* expression (25.5 ± 2-, 26 ± 5-, and 25 ± 8-fold activation of *espA*, *espC,* and *espD* expression, respectively, compared with Δ*phoP* carrying the empty vector p19Kpro). However, this was not the case when the mutant was complemented with *espB* (1.1 ± 0.1-, 0.9 ± 0.2-, and 0.8 ± 0.2-fold change of expression of *espA*, *espC,* and *espD*, respectively) or *espR* (3.3 ± 1.5-, 0.9 ± 0.2-, and 0.8 ± 0.2-fold change of expression of *espA*, *espC,* and *espD*, respectively). From these results we surmise the following: (i) PhoP contributes to ESX-1-dependent ESAT-6 secretion by activating *espACD* expression, and (ii) *espACD* overexpression in Δ*phoP M. tuberculosis* is sufficient to restore ESAT-6 secretion. Together, these data are in good agreement with previous findings reporting regulation of the *espACD* locus by PhoP (23, 27). However, these findings are in sharp contrast with recently reported results showing failure of the *espACD-TB* allele lacking RD8 (44) (a 5895-bp region covering a large part of the *espACD* promoter upstream of −464 relative to the start of the ORF; Fig. 3*D*) to complement ESAT-6 secretion in a Δ*phoPR* mutant of *M. tuberculosis* as opposed to the *M. bovis espACD* locus (36). These results suggested that the RD8 deletion, independent of *phoPR,* allows ESAT-6 secretion, and compensatory mutations in *M. bovis* help bypass the regulatory loop controlling *espACD* expression in *M. tuberculosis.* What remains to be understood is how the *M. tuberculosis* H37Rv PhoP regulates *espACD* and, in turn, critically contributes to ESAT-6 secretion.

Ectopic Expression of espACD Bypasses PhoP Functioning in Phagosome Maturation of M. tuberculosis H37Rv—Studies have shown the following: (i) ESX-1-dependent secretion of functional ESAT-6/CFP-10 contributes to inhibition of phagosome maturation (20, 45), and (ii) the attenuated *M. tuberculo-*

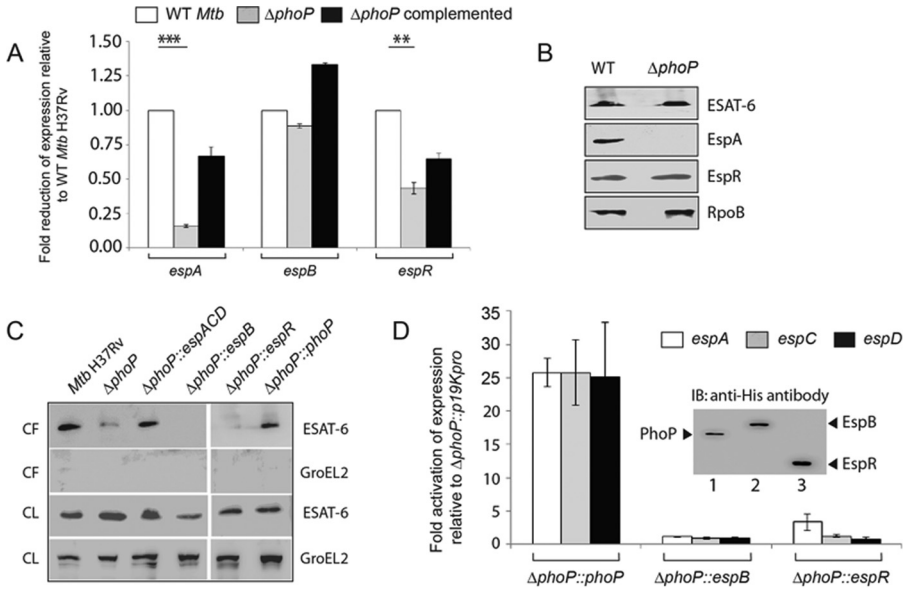

FIGURE 1. **PhoP-mediated *espACD* activation restores ESX-1-dependent ESAT-6 secretion of *M. tuberculosis*.** *A,* quantitative RT-PCR to examine expression levels of *espA*, *espB,* and *espR* in Δ*phoP* and Δ*phoP*-complemented strains relative to WT *M. tuberculosis* H37Rv. The results represent average values with standard deviations derived from at least three independent RNA preparations (*, $p < 0.05$; **, $p < 0.01$; ***, $p < 0.001$). *B,* immunoblot analyses of 20 μg of cell extracts of WT and Δ*phoP* using appropriate antibodies. RpoB was used as a loading control. *C,* immunoblot analyses of 20 μg of culture filtrates (*CF*) or cell lysates (*CL*) of indicated *M. tuberculosis* strains. αGroEL2 was used as a control to verify cytolysis of cells. Note that complementation of Δ*phoP M. tuberculosis* with *phoP*, *espB*, *espR,* and *espACD* was carried out using p19Kpro as the expression vector and compared with Δ*phoP M. tuberculosis* carrying p19Kpro as the empty vector control (see "Experimental Procedures"). *D,* expression of *espA*, *espC*, and *espD* in indicated mutant *M. tuberculosis*H37Rv strains relative to Δ*phoP-p19kpro* (empty vector control) as measured by RT-PCR analysis. *Inset* shows ectopic expression of proteins as detected by immunoblotting with anti-His antibody. *IB*, immunoblot.

TABLE 1
Strains and plasmids used in this study

Strain	Relevant genotype	Source or Ref.
E. coli DH5α	*recA1*;*endA1*;*gyrA96*; *thi*;*relA1*;*hsdR17* (*rK*−;*mK*+); *supE44*; *f80*Δ*lacZ*Δ*M15*;DlacZYA-*argF*; *UE169*	Novagen
E. coli BL21(DE3)	*fhuA2*[*lon*]*ompT gal* (λ*DE3*)[*dcm*]Δ*hsdS*λ*DE3*	Novagen
M. smegmatis mc^{2}155	Wild-type (WT) *M. smegmatis* strain	52
*Mtb*H37Rv	Wild-type (WT) *M. tuberculosis* strain	ATCC 25618
Δ*phoPMtb* H37Rv	Δ*phoP*::*attP-kan-attP*	Smith and co-workers (27)
Complemented Δ*phoPMtb* H37Rv	Δ*phoP*::pSM607	Smith and co-workers (27)
Plasmids		
pET-15b[a]	*E. coli* cloning vector	Novagen
pET-*phoP*	His_6-tagged PhoP expression plasmid	58
pET-*espR*	His_6-tagged EspR expression plasmid	This study
pET-28c[b]	*E. coli* cloning vector	Novagen
pET-*crp*	His_6-tagged CRP expression plasmid	This study
p19Kpro[c]	Mycobacteria expression vector	56
p19Kpro-*espACD*	Entire 1–3233 bp *espACD* operon cloned in p19Kpro	This study
p19Kpro-*espB*	EspB residues 1–460 cloned in p19Kpro	This study
p19Kpro-*espR*	EspR residues 1–132 cloned in p19Kpro	This study
p19Kpro-*phoP*	PhoP residues 1–247 cloned in p19Kpro	This study
pME1mL0031[b]	Mycobacterial protein expression vector	61
pME1mL1-*phoP*	PhoP residues 1–247 cloned in pME1mL1	This work
pSM128[d]	Integrative promoter probe vector for mycobacteria	57
pSM-espAup	espAup-*lacZ* fusion in pSM128	This work
pSM-espAupmut	Mutant espAup-*lacZ* fusion carrying changes in the PhoP-binding site	This work
pRSF-Duet-1[b]	*E. coli* cloning vector	Novagen
pRSF-Duet-*phoP-espR*	S-tagged PhoP and His-tagged EspR expression plasmid	This study
pUAB400 [b]	Integrative mycobacteria, *E. coli* shuttle plasmid	48
pUAB400-*phoP*	PhoP residues 1–247 cloned in pUAB400	55
pUAB300[c]	Episomal mycobacteria, *E. coli* shuttle plasmid	48
pUAB300-*espR*	EspR residues 1–132 cloned in pUAB300	This study
pUAB300-*phoR*	PhoR residues 1–485 cloned in pUAB300	55

[a] Amp^r is ampicillin resistance.
[b] Kan^r is kanamycin resistance.
[c] Hyg^r is hygromycin resistance.

sis H37Ra strain is impaired for ESAT-6 secretion due to a point mutation in the C-terminal DNA binding domain of PhoP (23). These studies were extended to examine the effect of infection of dendritic cells (DCs) with *M. tuberculosis* H37Ra and recombinant H37Ra complemented with a copy of the *phoP* gene (Rv0757), which restores ESAT-6 secretion and elicits specific T-cell responses (23). Consistent with earlier results, infection of DCs with *M. tuberculosis* H37Ra matured into phagolysosomes; however, infection of DCs with H37Ra::*phoP* inhibited phagosome maturation (46). To set up our experimental model, we infected murine macrophages with WT *M. tuberculosis* H37Rv and indicated mutant strains. As expected, WT *M. tuberculosis* H37Rv inhibited phagosome maturation (Fig. 2), whereas phagosomes with Δ*phoP M. tuberculosis* H37Rv

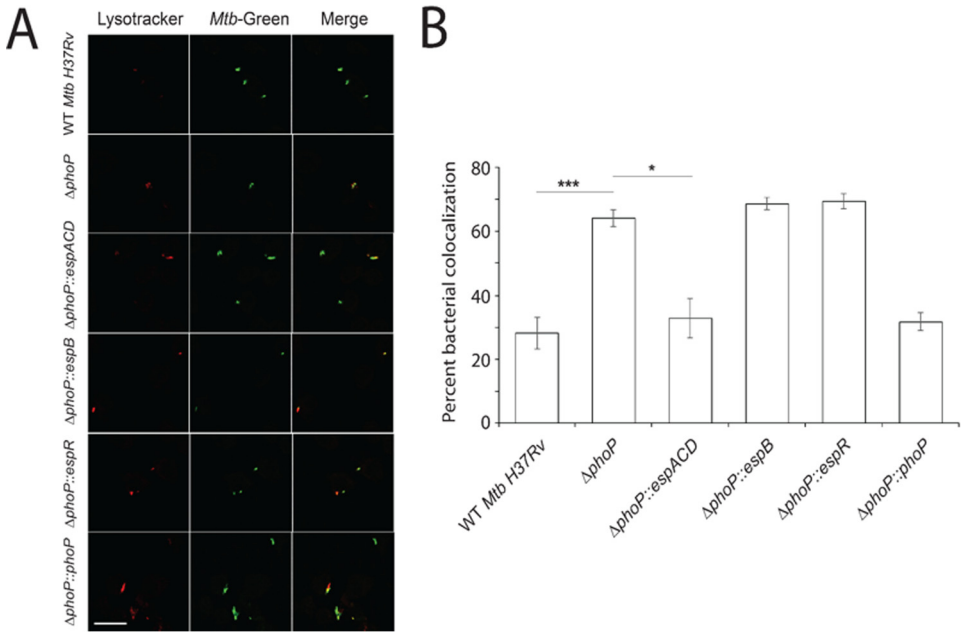

FIGURE 2. **PhoP-dependent *espACD* activation is required for inhibition of phagosome maturation by *M. tuberculosis* H37Rv.** *A,* macrophages were infected with WT or indicated mutant strains of *M. tuberculosis* H37Rv for 3 h. The cells were stained with 300 nM LysoTracker for 3 h and then fixed in 4% paraformaldehyde. *M. tuberculosis* H37Rv strains were labeled with fluorescent phenolic auramine. The confocal images represent the merge of two fluorescence signals (LysoTracker, *red*; *M. tuberculosis, green*) and are shown at *right*. *Scale bar,* 10 μm. *B,* percent bacterial co-localization for indicated *M. tuberculosis*H37Rv strains. The results show the average values with standard error of mean (S.E.) of at least three independent experiments (*, $p < 0.05$; ***, $p < 0.001$).

matured into phagolysosomes. Remarkably, Δ*phoP* expressing *espACD* could restore its ability to inhibit phagosome maturation at the level of the WT *M. tuberculosis*. In contrast, this was not the case for the Δ*phoP* strains expressing *espB* and *espR*. Thus, from bacterial co-localization data, we conclude that ectopic expression of *espACD* can bypass PhoP function, which inhibits phagosome maturation via ESAT-6 secretion of *M. tuberculosis* H37Rv.

Recruitment of PhoP and EspR at the espACD Promoter—We next examined whether PhoP is recruited at the *espACD* promoter. To this end, the full-length promoter region (espAup) was divided into the following four parts, espAup1–up4 (Fig. 3*A*), and ChIP-qPCR was attempted using anti-PhoP antibody. Our results show that in contrast to espAup1 and espAup3, espAup2 and espAup4 showed 7.2 ± 0.7- and 3.3 ± 0.7-fold enrichments, respectively, in the anti-PhoP IP compared with the mock sample lacking an antibody (Fig. 3*B*). Thus, PhoP is recruited at specific sites within the *espACD* promoter. It should be noted that partly consistent with these results, a recent report suggests PhoP binding to a region that maps within espAup4 spanning +60 to −245 relative to the translation start site of the ORF (37). However, under the conditions we examined, espAup2 reproducibly showed the highest level of PCR enrichment in ChIP experiments (Fig. 3). As EspR was shown to bind to *espACD* and activate its expression (29, 38, 40), we also examined EspR recruitment to espAup. In agreement with previously published results (38), espAup2 showed PCR enrichment of 12 ± 3.0-fold in anti-EspR IP relative to the mock sample lacking an antibody (Fig. 3*C*). Together, these results suggest that within the *espACD* promoter EspR is specifically recruited proximal to the PhoP-binding site. Based on preliminary bioinformatics analysis and our knowledge on recently reported PhoP-binding consensus sequence, we propose the region spanning −787 to −770 as the likely target site of PhoP within espAup2. It should be noted that He and Wang (37) have recently identified a PhoP-binding site upstream of *espACD,* and the nucleotide sequence spans from −214 to −197 relative to the start of the ORF. Fig. 3*D* summarizes the above results showing the *espACD* regulatory region with relevant protein-binding sites, including the newly shown PhoP-binding site within espAup2 (as shown above) in conjunction with previously known PhoP- and EspR-binding sites. Notably, EspR has previously been shown to bind to the regulatory region of *espACD* at −468, −798, and −983, which are located within espAup3, espAup2, and espAup1, respectively (Fig. 3*A*). However, results reported in this study suggest that EspR seems to be almost comparably recruited to espAup1, espAup3, and espAup4 (Fig. 3*B*). Although both studies involved ChIP experiments to assess EspR binding, the fact that an anti-EspR antibody was used in our assays *versus* anti-FLAG antibody used by Rosenberg *et al.* (38) and important differences in the conditions of ChIP assays most likely account for this discrepancy. To examine whether PhoP recruitment to the upstream regulatory region of *espACD* has any regulatory effect on the expression of adjacent *Rv3617*, we compared expression levels of *Rv3617* between WT *M. tuberculosis* H37Rv and Δ*phoP M. tuberculosis* H37Rv by RT-PCR (supplemental Fig. S2). The results show that the *phoP* locus does not appear to regulate *Rv3617* expression in *M. tuberculosis* H37Rv.

Probing PhoP Binding to the espACD Promoter—To examine the PhoP-binding site more closely, a number of espAup2-derived promoter fragments (espAup2a–2e) were amplified (Fig. 4*A*). EMSA experiments using the end-labeled fragments show that PhoP binds to espAup2a spanning −957 to −700 (relative

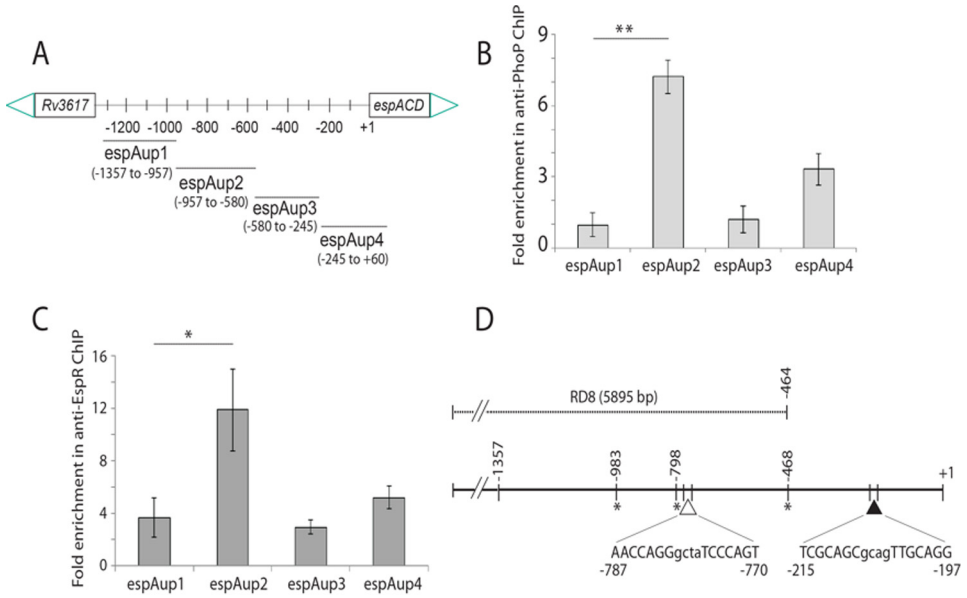

FIGURE 3. **Recruitment of PhoP and EspR at the *espACD* promoter.** *A,* scheme showing organization of the *espACD* promoter divided into four fragments (espAup1–espAup4) to probe PhoP and EspR binding. Note that the promoter fragments espAup1–espAup4 span from −957 to −1357, −580 to −957, −245 to −580, and +60 to −245, respectively, relative to the start site of the ORF. To examine PhoP (*B*) and EspR (*C*) recruitment within the *espACD* promoter, ChIP-qPCR was carried out as described under the "Experimental Procedures." Each data point represents mean of duplicate qPCR measurements using at least three independent *M. tuberculosis* cultures. *Asterisk* indicates a statistically significant difference in the ChIP enrichment level compared between espAup1 and espAup2 under the conditions examined (*, $p < 0.05$; **, $p < 0.01$). Note that the difference in the signal enrichment between PhoP and EspR antibodies may be attributable to affinity differences between proteins and/or respective antibodies. *D,* location of relevant protein-binding sites within *espACD* upstream regulatory region. Note that the EspR-binding sites, indicated by *asterisks*, are known to be centered around −468, −798, and −983 (relative to the start site of the ORF) (38), and the only reported PhoP-binding site shown by a *filled triangle* spans from −215 to −197 (37). However, the PhoP-binding site revealed in this study, shown by an *empty triangle*, spans from −781 to −770 based on sequence similarity with the consensus PhoP-binding motif (37). Importantly, the region upstream of −464, as shown in figure, constitutes part of RD8, including both the PhoP- and EspR-binding sites relevant to *espACD* activation.

to the start site of the ORF) and remains ineffective to form a stable complex to other parts of espAup2 (Fig. 4*B*). Additional EMSA experiments assessed the specificity of PhoP binding to espAup2a using a large excess of specific and nonspecific competitors in the binding mix (Fig. 4*C*). The results clearly show that low affinity PhoP binding to espAup2a is sequence-specific. Importantly, these results are consistent with the proposed PhoP-binding site spanning −787 to −770 (see Fig. 3*D*). To examine the role of this motif, mutations were introduced into both of the repeat units (DRu1 and DRu2) of espAup as shown in Fig. 4*G*. We next carried out PhoP-dependent transcriptional regulation of WT and mutant espAup in *Mycobacterium smegmatis*. For reporter assays as described in Fig. 4*H*, although the construct carrying WT promoter (espAup-*lacZ*) reproducibly showed 2.40 (±0.6)-fold promoter activation with induction of PhoP, espAupmut-*lacZ* displayed largely comparable β-galactosidase activity (1.2(±0.3)-fold difference) when compared in cell extracts of *M. smegmatis* with or without induction of *M. tuberculosis* PhoP. Thus, we surmise that PhoP recruitment to the above-noted direct repeat motif within espAup2 is necessary and sufficient for PhoP-coupled transcription regulation of espAup. As expected, PhoP from *M. tuberculosis* H37Ra (referred to as H37Ra, PhoP), which carries an S219L point mutation at the C-terminal effector domain (25, 26, 47) and was unable to restore ESAT-6 secretion upon complementation of Δ*phoP M. tuberculosis* H37Rv (23), failed to show effective DNA binding to end-labeled espAup2a compared with PhoP from *M. tuberculosis* H37Rv (supplemental Fig. S3). Strikingly, one of the EspR-binding sites at the *espACD* promoter is centered at −798, *i.e.* within espAup2a (38). Thus, *M. tuberculosis* EspR was expressed and purified as shown in supplemental Fig. S4*A*. To verify DNA binding function of the recombinant protein, purified EspR was used in EMSA experiments with end-labeled espAup2a. In agreement with previously published results, EspR showed sequence-specific binding to end-labeled espAup2a (supplemental Fig. S4*B*).

Having shown that both PhoP and EspR bind to espAup2a, we wished to investigate whether both the regulators can together bind to epsAup2a. Notably, at relatively lower protein concentrations both PhoP (*lanes 2* and *3*, Fig. 4*D*) and EspR (*lanes 4* and *5*, Fig. 4*D*) showed inefficient binding to end-labeled espAup2a. In contrast, the presence of both PhoP and EspR under identical conditions showed a striking stimulation of >20-fold of DNA binding (based on limits of detection in these assays) concomitant with the formation of a single retarded complex (Fig. 4*D, lanes 6* and *7*). However, a similar experiment using purified PhoP and CRP (also known to have regulatory influence on the *espACD* expression (28)) together under identical conditions failed to generate a complex stable to electrophoresis (Fig. 4*D, lanes 10* and *11*). Note that CRP, with its DNA-binding site 1049-bp upstream of the start site of *espACD* ORF (see *espAup1*; Fig. 3*A*) (28) in the vicinity of espAup2a (−957 to −700; see Fig. 4*A*) was chosen as a control protein. This is because other DNA binding regulators of *espACD* expression, for example MprA and WhiB6, display binding downstream of espAup2 (31, 32), and until now, the Lsr2-binding site within the *espACD* promoter remains unknown. Functionality of recombinant CRP was demon-

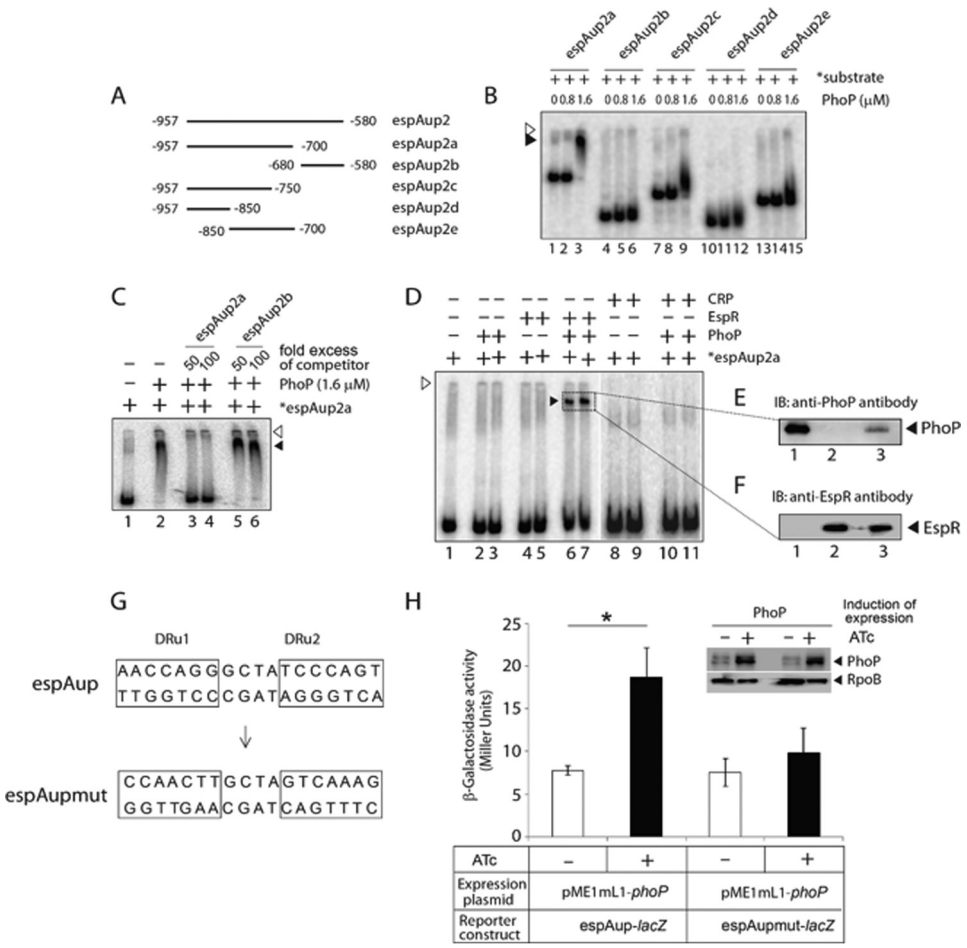

FIGURE 4. **Probing *in vitro* binding of PhoP and EspR to the *espACD* regulatory region.** *A,* to probe the core binding site of PhoP within espAup2, indicated promoter fragments (espAup2a–espAup2e) were amplified and end-labeled as described under "Experimental Procedures." *B,* EMSA of radiolabeled espAup2-derived promoter fragments with indicated concentrations of *M. tuberculosis* PhoP shows that the regulator directly binds to espAup2a comprising −957 to −580 of the regulatory region relative to the ORF start site. *C,* specificity of binding was examined by EMSA in the presence of 50- and 100-fold excess of indicated specific and nonspecific competitors. *D,* EMSA of end-labeled espAup2a to examine binding of PhoP (0.4 and 0.8 μM in *lanes 2* and *3*, respectively), EspR (0.1 and 0.2 μM in *lanes 4* and *5*, respectively), and both PhoP (0.4 and 0.8 μM) and EspR (0.2 μM each) together in *lanes 6* and *7*, CRP (0.1 and 0.2 μM in *lanes 8* and *9*, respectively), and both PhoP (0.4 and 0.8 μM) and CRP (0.2 μM each) together in *lanes 10* and *11*, respectively, were carried out as described under the "Experimental Procedures." In all cases the position of the radioactive material was determined by exposure to a phosphor-storage screen, and bands were quantified by a phosphorimager (Fuji). The *empty* and *filled arrowheads* indicate the wells (at the origin) and the position of the retarded probe, respectively. *E* and *F*, to examine the composition of the retarded complex (shown by *filled triangles*), the relevant band (shown inside the *box*) representing the complex was excised; protein components were extracted and resolved by SDS-PAGE, and immunoblotted with appropriate antibodies; *lane 1* (*E*) and *lane 2* (*F*) resolve recombinant PhoP and EspR, respectively, as positive controls, and *lane 3* (for both *E* and *F*) resolves protein sample eluted from the retarded complex. *IB,* immunoblot. *G,* nucleotide sequences of the proposed PhoP-binding direct repeat motif consisting of the upstream and downstream repeat units (*DRu1* and *DRu2*, respectively). To construct the mutant promoter espAupmut, changes in both the repeat units were introduced by changing As to Gs and Cs to Ts and vice versa, and the orientation of the DRu2 sequence was then reversed relative to DRu1 (see "Results" for details). Note that the espAupmut represents espAup fragment carrying changes only at the proposed PhoP-binding site. *H,* PhoP regulates expression of espAup by specific recognition of the direct repeat motif. WT *M. smegmatis* harboring espAup-*lacZ* and espAupmut-*lacZ* fusions were grown, and β-galactosidase activities with or without inducing *M. tuberculosis* PhoP expression were measured at 24-h time point as described earlier (54). The results show the average values with standard error of mean (S.E.) of at least two independent experiments (*, $p < 0.05$). *Insets* compare expression of PhoP in crude extracts containing equal amounts of total protein by Western blotting using anti-PhoP antibody. As loading control, crude extracts were probed with anti-RpoB antibody (Abcam).

strated by high affinity DNA binding to the espAup1 promoter fragment (supplemental Fig. S5). Upon elution of protein components from the single retarded complex (Fig. 4*D*, *lanes 6* and *7*) and subsequent immunoblotting analysis (Fig. 4, *E* and *F*), we confirmed identity of the slower moving band as the PhoP-EspR-DNA ternary complex. Having shown that PhoP binds to espAup2a, we have compared *in vitro* binding efficiency of PhoP to espAup2a and espAup4 (supplemental Fig. S6), the other target site of PhoP within *espACD* upstream regulatory region (see Fig. 3*D*) (37). Our results indicate that compared with espAup2, PhoP on its own appears to bind to espAup4 with ~2–3-fold higher affinity. Although the result appears contradictory to what we observed in ChIP experiments (Fig. 3*D*), we hypothesize that PhoP binding to these two sites presumably account for two different regulatory mechanisms most likely involving different affinities. Note that PhoP-binding site within espAup4 is part of the espACD-TB allele that was unable to restore ESAT-6 secretion in Δ*phoPR M. tuberculosis* H37Rv (36).

EspR Recruitment to espACD Promoter Requires the Presence of PhoP—We next compared EspR recruitment in WT and Δ*phoP* by ChIP-qPCR (Fig. 5*A*) using anti-EspR antibody as described above. Remarkably, in the case of the Δ*phoP* mutant, we observed significantly reduced PCR enrichment of espAup2

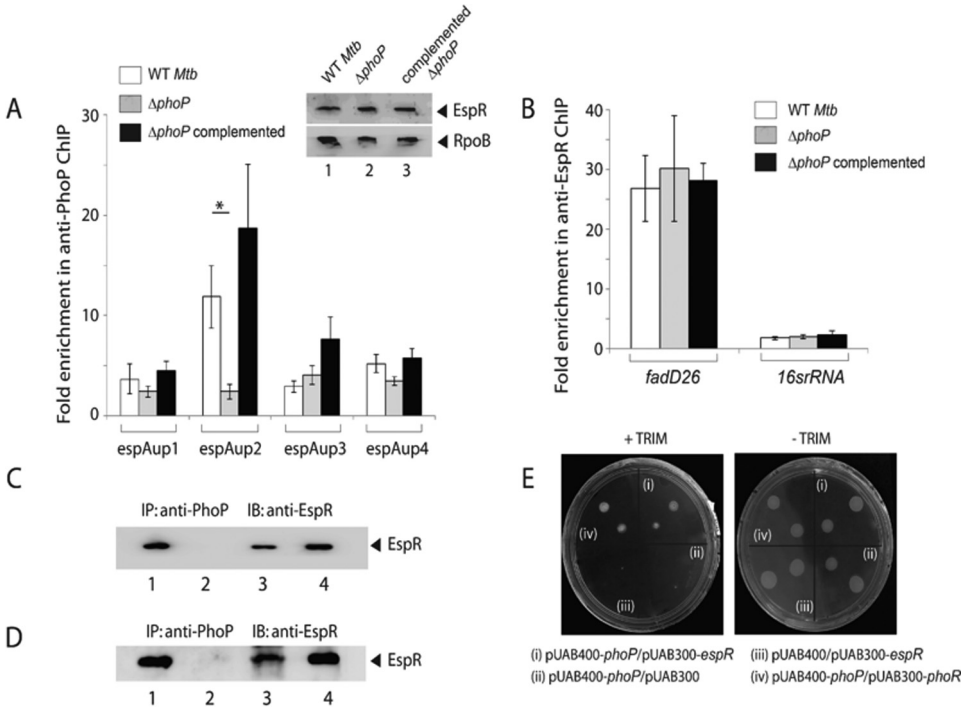

FIGURE 5. **Recruitment of EspR at the *espACD* promoter requires the presence of PhoP.** *A,* ChIP-qPCR was carried out to assess EspR recruitment to the *espACD* promoter of WT, Δ*phoP,* and the complemented mutant. Fold PCR enrichment due to EspR binding was determined against PCR signal from the mock sample generated by an IP experiment without adding antibody. Note that anti-EspR ChIP data of Fig. 3*C* was included here to enable a direct comparison of results from WT and Δ*phoP M. tuberculosis*. Each data for ChIP experiments represent the mean of duplicate qPCR measurements using at least three independent *M. tuberculosis* cultures. *Asterisk* indicates a statistically significant difference in the ChIP enrichment at espAup2 compared between WT *M. tuberculosis* and the *phoP* mutant (*, $p < 0.05$). *Inset* shows comparable EspR expression in WT, Δ*phoP,* and complemented Δ*phoP* as determined by immunoblotting of crude cell lysates (~20 μg of total protein) using anti-EspR antibody; RpoB was used as a loading control. *B,* to examine specificity of *in vivo* EspR recruitment, ChIP-qPCR experiments utilized *fadD26* promoter as a positive control using appropriate primer pair (supplemental Table S2). Specificity of enrichment was also verified with 16S rRNA gene-specific primer (supplemental Table S2) using identical anti-EspR IP samples from the WT and the mutant *M. tuberculosis* strains. *C,* to examine PhoP-EspR interaction *in vivo*, crude cell lysates of WT *M. tuberculosis* H37Rv were immunoprecipitated with anti-PhoP antibody, and IP samples were visualized by immunoblotting with anti-EspR antibody; *lane 1*, input sample; *lane 2*, control with mock IP (without adding antibody), *lane 3*, anti-PhoP IP of crude lysate, and *lane 4,* recombinant EspR as a positive control. *D,* to further examine PhoP-EspR interaction *in vitro*, crude cell lysates of *E. coli* BL21(DE3) expressing both PhoP and EspR via pRSF-Duet-1 vector as described under the "Experimental Procedures" was immunoprecipitated with anti-PhoP antibody, and IP samples were visualized by Western blot analysis using anti-EspR antibody. The lane composition of the SDS-PAGE remains identical to that of *C*. *E,* M-PFC experiment to study interaction of PhoP and EspR involved co-expression of indicated fusion constructs in *M. smegmatis*, used as a surrogate host. Growth of transformants on 7H10/kanamycin/hygromicin hygromycin in presence of TRIM confirms *in vivo* protein-protein association between PhoP and EspR. Co-expression of empty vectors and *phoP*/*phoR* pair were included as negative and positive control, respectively. All of these strains grew well in absence of TRIM. *IB*, immunoblot.

relative to WT *M. tuberculosis* (compare 12 ± 3-fold *versus* 2.4 ± 0.6-fold). However, *fadD26,* which is directly regulated by EspR (42) but not by PhoP (41), showed comparable EspR recruitment in the WT and the mutant (Fig. 5*B*), suggesting that specific EspR recruitment to the *espACD* promoter is dependent on the presence of PhoP. Notably, we observed comparable EspR expression in WT, Δ*phoP,* and complemented Δ*phoP* as determined by immunoblotting of crude cell lysates (~20 μg of total protein) with anti-EspR antibody (*inset* to Fig. 5*A*). It should be noted that the specificity of recruitment as determined by ChIP experiments in anti-EspR IP was also verified by using *16srRNA* gene-specific primers (Fig. 5*B*). Having found that recruitment of EspR required the presence of PhoP, we sought to investigate whether PhoP interacts with EspR. To this effect, *M. tuberculosis* cell extract was immunoprecipitated by anti-PhoP antibody (as described under "Experimental Procedures"), and IP samples were probed with anti-EspR antibody (Fig. 5*C*). Although the mock sample lacking an antibody could not detect EspR (Fig. 5*C, lane 2*), the anti-PhoP IP clearly detected the presence of EspR (*lane 3*), suggesting *in vivo* interaction between PhoP and EspR. To investigate whether the target DNA site contributes to PhoP-EspR protein-protein interactions in co-immunoprecipitation experiments, we expressed both PhoP and EspR in *Escherichia coli* BL21(DE3) via pRSF-Duet-1 vector as described under "Experimental Procedures." Next, the crude cell lysate was immunoprecipitated with anti-PhoP antibody as described above, and IP samples were visualized by Western blot analysis using anti-EspR antibody (Fig. 3*D*). Our results suggest that *M. tuberculosis* PhoP and EspR when co-expressed in *E. coli* are also capable of interacting with each other. We further studied PhoP-EspR interaction using the mycobacterial protein fragment complementation (M-PFC) assay as described previously (Fig. 5*D*) (48). Interestingly, in the presence of 15 μg/ml TRIM, *M. smegmatis* co-expressing *M. tuberculosis* PhoP and EspR grew just as well compared with cells co-expressing PhoP and PhoR (used as positive control). In contrast, cells containing empty vectors showed no growth on 7H10/TRIM plates, although all of the *M. smegmatis* strains grew well in the absence of TRIM. From these results, we conclude specific protein-protein interaction(s) between *M. tuberculosis* PhoP and EspR in *M. smegmatis*.

Discussion

The presence of the RD1-encoded ESX-1 locus in both pathogenic and nonpathogenic species indicates that it may not be solely involved in virulence of *M. tuberculosis*. In fact, ESX-1 was shown to regulate DNA conjugation of the nonpathogenic *M. smegmatis* (49, 50). In contrast, the *espACD* operon is absent in *M. smegmatis* (43) and is perhaps indicative of its direct role in virulence mechanisms. In agreement with these results independent of its role as a secreted protein, EspA functions as a critical mediator of ESX-1-dependent virulence regulation (22). It is noteworthy that EspR, the major regulator of the *M. tuberculosis* ESX-1 protein secretion system, has been shown to be a nucleoid-associated protein with the ability to bind 165− loci of the bacterial genome (42). We show here that the regulatory region of *espACD* constitutes a major target by which the virulence regulator PhoP critically modulates ESAT-6 secretion (Fig. 1). Remarkably, our results suggest that simultaneous recruitment of PhoP and EspR at the *espACD* regulatory region, controlled by PhoP-EspR protein-protein interactions, contributes to *espACD* activation, which in turn regulates ESAT-6 secretion. These results account for an explanation of how EspR-dependent activation of *espACD* (29) is linked to positive regulation of the same operon by PhoP. In agreement with these results, PhoP is shown to regulate phagosome maturation via *espACD* activation-dependent ESAT-6 secretion (Fig. 2). Together, these results showing a complex interplay of two virulence regulators to control ESX-1-dependent ESAT-6 secretion have significant implications on the mechanism of virulence regulation of *M. tuberculosis*.

It should be noted that *espR* expression has been suggested to be under the direct control of PhoP (27, 39). Strikingly, our results reveal that PhoP is recruited in the vicinity of EspR-binding site (Figs. 3 and 4 and supplemental Fig. S2*B*), and there is synergistic DNA binding activity of the two regulators at the *espACD* regulatory region (Fig. 4). However, it remains unclear whether PhoP serves to stabilize EspR. Considering the proximal site(s) of action and synergistic DNA binding activity, it was of interest to understand whether these regulators are functionally connected. These considerations take on more significance in the light of previous results showing that espAup2a comprises the EspR-binding B-site (centered at −798), which binds cooperatively with the C-site (centered at −983) and generates DNA looping to assist transcription initiation (Fig. 6) (38, 40). These results are suggestive of a critical role of PhoP in binding and transcriptional control of *espACD* operon in association with EspR. In agreement with this notion, remarkably EspR was unable to be recruited at the *espACD* promoter in the *phoP* mutant of *M. tuberculosis* (Fig. 5). We further extended the study to show that PhoP-EspR protein-protein interaction (Fig. 5) accounts for concomitant binding of both the regulators at the *espACD* regulatory region. Although the proposed model shows an equimolar PhoP and EspR in the ternary complex, we do not have direct evidence to suggest a 1:1 binding ratio of PhoP and EspR in the model. However, the mechanism of DNA binding by both PhoP and EspR, as independent regulators, has been investigated in great detail, and in both cases a dimer of PhoP or EspR has been suggested to bind DNA (37, 40, 51).

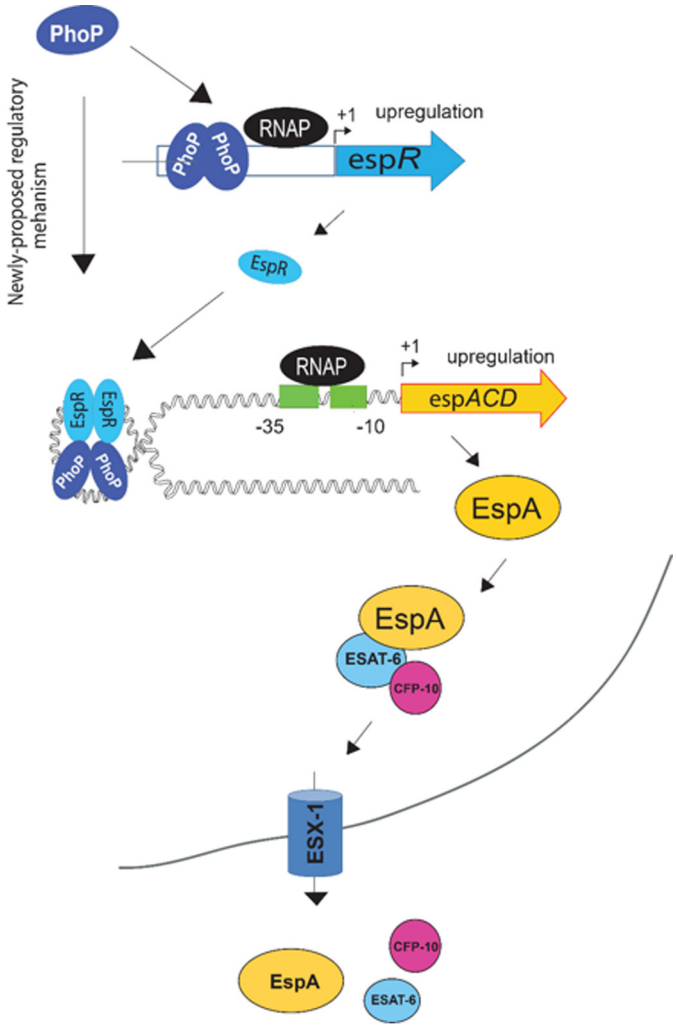

FIGURE 6. **Schematic model showing newly proposed mechanism of activation of *espACD* expression by simultaneous binding of PhoP and EspR.** It should be noted that EspR upon binding to DNA has been suggested to form hairpin-like structures (40). Here, we propose that the additional stability of the higher order complex is perhaps attributable to protein-protein interaction between PhoP and EspR. The proteins remain bound to their target sites away from the transcription start site allowing RNA polymerase to initiate transcription. Notably, EspA and EspC proteins are themselves substrates for the ESX-1 secretion system co-secreting ESA-6 and CFP-10.

Thus, the differential requirement to form a ternary complex (Fig. 4*D*) or apparent differences in the amounts of proteins in the complex (Fig. 4, *E* and *F*) may simply be attributable to a difference in concentration of "active fractions" of proteins in the respective preparations.

Although recent reviews implicate PhoP and EspR in controlling the *espACD* genes in the context of regulation of ESAT-6 secretion (33, 34), the mechanism of *espACD* regulation remains unknown. Also, what remains puzzling is why an extra copy of the *espACD-TB* allele could not restore ESAT-6 secretion of Δ*phoPR M. tuberculosis* (36). As noted above, our results show that (i) identification of PhoP binding to espAup2 (−787 to −770 within RD8; Fig. 3*D*) proximal to previously determined EspR-binding site (Fig. 3), (ii) PhoP-EspR-*espACD* ternary complex formation (Fig. 4), and (iii) *in vivo* recruitment of PhoP and EspR controlled by protein-protein interactions (Fig. 5) clearly demonstrate the importance of RD8 in PhoP-

EspR-*espACD* regulatory loop, a major player in *phoP*-dependent ESAT-6 secretion. Together, these results account for an explanation of why *M. tuberculosis espACD*-allele lacking RD8 could not restore ESAT-6 secretion of Δ*phoPR M. tuberculosis*.

Given the fact that EspR binds to at least 165 loci on the *M. tuberculosis* genome as a global nucleoid-associated protein (42), the finding that PhoP remains a prerequisite to ensure specific recruitment of EspR within the *espACD* promoter offers a new mechanistic insight into the regulation of the ESX-1 secretion system. Such a situation might allow PhoP to function efficiently, by ensuring that EspR only binds to the *espACD* promoter already bound to PhoP. It is possible that recruitment of PhoP changes DNA conformation (as it binds), which subsequently facilitates recruitment of EspR, a protein capable of participating in long range interactions (38, 40). Thus, a DNA-dependent complex interplay of PhoP and EspR likely contributes to the precise regulation of the *espACD* operon, which perhaps is appropriate for an operon that plays such a critical role in the virulence mechanisms of *M. tuberculosis* (43). Clearly, as speculated in the schematic model (Fig. 6), PhoP-EspR protein-protein interaction appears to contribute additional stability to the higher order structure to provide access to RNA polymerase for transcription initiation.

In *M. tuberculosis*, most likely the ESX-1 secretion system is under precise regulation because the secreted proteins, although essential for a successful infection, are strongly antigenic, and their deregulated secretion is likely to alert the immune system to the infection. Thus, a rather complicated regulation of the ESX-1 system during infection may be achieved through integration of multiple regulators. However, given the importance of the upstream control region of *espACD* operon, such a regulatory mechanism is unlikely to be applicable to other members of the *M. tuberculosis* complex. This is because the regulatory region of *espACD* for the closely related *M. bovis* includes 456 bp only (43), and for other members of the *M. tuberculosis* complex, the *espACD* promoter is even shorter arguing for a simpler transcription regulation without involving multiple regulators. Nevertheless, results reported in this work showing recruitment of a nucleoid-associated protein (as a functional partner) by a key regulator represents an additional layer of complexity that has perhaps evolved to further tune niche-specific gene expression. It is possible that to achieve precisely coordinated regulation of a specific gene's expression, and this may be a more common mechanism exploited by prokaryotic organisms than has been previously recognized.

Experimental Procedures

Bacterial Strains and Growth Conditions—E. coli DH5α and BL21(DE3) served as the host for routine cloning and overexpression of recombinant forms of proteins, respectively. *M. smegmatis* mc^{2}155, an electroporation-efficient strain (52), and all of the *M. tuberculosis* strains used (Table 1) were grown in liquid 7H9 broth (Difco) supplemented with 0.2% glycerol, 0.05% Tween 80, and 10% albumin/dextrose/catalase or on 7H10-agar medium (Difco) containing 0.5% glycerol and 10% oleic acid/albumin/dextrose/catalase enrichment supplemented with 20 μg/ml kanamycin, 50 μg/ml hygromycin, or 20 μg/ml streptomycin, as appropriate. For secretion analysis, *M. tuberculosis* strains were grown in Sauton medium. Δ*phoP M. tuberculosis* H37Rv and the complemented mutant strains were kind gifts from Dr. Issar Smith and have been described elsewhere (27). Briefly, Δ*phoP* of *M. tuberculosis* was generated by disrupting the *phoP* gene via insertion of kanamycin-resistant cassette from pUC-K4 into a unique EcoRV site and confirmed by Southern blot analysis. Plasmids were electroporated into wild type (WT) or mutant strains by standard protocol (53). pSM607 containing a 3.6-kb DNA fragment of *M. tuberculosis phoPR,* including the 200-bp *phoP* promoter region, a hygromycin-resistant cassette, the *attP* site, and the gene encoding phage L5 integrase, was transformed into the *phoP* mutant to complement *phoP* expression.

Cloning, Bacteria Preparation, and Culture Filtrate Analysis—Plasmid DNA isolation, restriction digestion, and electrophoresis by agarose gels were carried out by standard protocol as described previously (54, 55). To express *phoP*, *espB*, *espR,* and *espACD* in Δ*phoP M. tuberculosis*, appropriate ORFs were cloned in p19KPro (56) using primer pairs FPphoP19K/RPphoP19K, FPespB19K/RPespB19K, FPespR19K/RPespR19K, and PespACD19K/RPespACD19K, respectively (supplemental Table S1). Plasmids were transformed in Δ*phoP M. tuberculosis* by electroporation, and 100 ml of transformed cells were grown to mid log phase (A_{600} = 0.6–0.8). Bacterial cells were centrifuged, washed twice in PBS, and resuspended in 500 ml of Sauton medium. Cells were grown further at 37 °C for 4–5 days, and cultures were harvested to obtain culture filtrates and cell pellets. For culture filtrate analyses, the cell pellet was removed, and culture filtrates were successively filtered through 0.45- and 0.22-micron filters to remove any residual cells and concentrated by ammonium sulfate precipitation. For cell lysates, cells were resuspended in lysis buffer (PBS containing a protease inhibitor mixture, Roche Applied Science) and lysed in the presence of silica beads (100 μm Lysing matrix B, MP Biomedicals) in a FastPrep at a speed setting of 5.5 for four times for 25 s. The supernatant was collected by centrifugation and filtered through a low-binding Millex 0.22-μm membrane filter (Millipore). In all cases an aliquot of cell lysate and culture filtrate was used to determine protein concentration using BCA protein estimation kit (Pierce).

Transcriptional fusions to *lacZ* were obtained by cloning PCR-amplified fragments of the *M. tuberculosis espA* regulatory region (espAup) into the ScaI site of pSM128 (a promoterless integrative *lacZ* reporter vector (57) with a streptomycin resistance gene) using a primer pair FPespAup1/RPespAup4 (supplemental Table S1). The espAup comprised 1357-bp upstream of the coding region and included the first 60 coding bases of the *espA* gene. To examine the importance of the PhoP-binding direct-repeat motif within the *espA* promoter, sequence variants that were altered in both the repeat units were generated using a two-stage overlap extension method by interchanging all the As with Cs, all the Gs with Ts, and finally turning around the downstream repeat unit (see supplemental Table S1 for mutagenic primer pair FPespAmut/RPespAmut). In all cases, *lacZ* transcriptional fusion constructs were verified by DNA sequencing.

Reporter Assays in M. smegmatis—Electro-competent *M. smegmatis* transformed with pME1mL1-*phoP* expressed *M. tuberculosis* PhoP from the P_{myc1}*tet*O promoter under the control of the TetR repressor as described previously (54). Cultures of *M. smegmatis* strains harboring indicated *lacZ* fusions and the PhoP expression construct (or no expression plasmid as control) were grown in the absence or in presence of 50 ng/ml anhydrotetracycline, used as an inducer of PhoP expression. Promoter activation with induction of PhoP expression was assessed by measuring β-galactosidase activity (in Miller units) of crude cell lysates as detailed earlier (54). TetR-controlled PhoP expression in crude lysates of *M. smegmatis* (≈5 μg of protein) was verified by Western blot analysis using anti-PhoP antibody (Alpha Omega Sciences, India).

Expression and Purification of Recombinant Proteins—Recombinant PhoP from *M. tuberculosis* H37Rv and *M. tuberculosis* H37Ra, referred to as PhoP and H37Ra.PhoP, respectively, were expressed in *E. coli* and purified as described previously (58). To express *M. tuberculosis* EspR, the coding region of the *espR* gene (Rv3849) extending from Met-1 to Lys-141 was PCR-amplified from *M. tuberculosis* H37Rv genomic DNA. The primer pair espRstart/espRstop (supplemental Table S1) introduced an NdeI site at the start codon and a BamHI site 3′ of the stop codon, respectively. The PCR-derived fragment was gel-purified, restricted with NdeI and BamHI, and ligated to the NdeI/BamHI backbone fragment of pET15b (Novagen) to generate full-length EspR protein with an N-terminal His_6 tag (pET-EspR). To express recombinant *M. tuberculosis* CRP from *E. coli*, the coding region of the gene (Rv3676) comprising 224 amino acid residues was PCR-amplified from *M. tuberculosis* H37Rv genomic DNA using the crpStart/crpStop (Table S1) primer pair. The PCR-derived fragment was cloned between NdeI and HindIII sites of pET28c (Novagen) to generate full-length CRP protein with a C-terminal His_6 tag (pET-*crp*). The construct was verified by DNA sequence analysis.

To purify His_6-tagged EspR, cell lysates overexpressing EspR was loaded onto a nickel-nitrilotriacetic acid (Qiagen)-agarose for affinity purification. Proteins were eluted using a gradient of imidazole in 50 mM Tris-HCl (pH 7.9), 500 mM NaCl, 10% glycerol, and 15 mM imidazole. The peptide content of the column fractions was analyzed by SDS-PAGE, and Coomassie Brilliant Blue was used to stain protein bands. Recombinant EspR was recovered predominantly in the 250 mM imidazole eluate. Eluted protein was dialyzed overnight in 50 mM Tris-HCl (pH 7.9), 200 mM NaCl, 10% glycerol and stored at −80 °C. Recombinant *M. tuberculosis* CRP was purified following an identical protocol as that of PhoP. Protein contents were determined by BCA protein estimation reagent with bovine serum albumin as the standard and compared with values obtained from Quant-iT protein assay kits and Qubit fluorometer (Invitrogen). The approximate yield of purified proteins was ~8–10 mg pf protein/liter of culture. In all cases, protein concentrations are given in equivalents of protein monomers.

EMSA—Purified recombinant proteins PhoP and EspR were used to assess protein binding to various *espACD* promoter fragments, generated by PCR from espAup, resolved on agarose gels, and recovered by gel extraction. The fragments were end-labeled with [γ-^{32}P]ATP (1000 Ci nmol^{-1}) using T4 polynucleotide kinase and purified from free label by Sephadex G-50 spin columns (GE Healthcare). Indicated concentrations of purified proteins were incubated with appropriate end-labeled probes in a total volume of 10 or 20 μl of binding mix, and DNA-protein complexes were resolved by electrophoresis on a 6% (w/v) non-denaturing polyacrylamide gel as described previously (55). To examine specificity of binding, unlabeled specific and nonspecific competitor DNA at indicated molar excess was incubated with purified proteins for 10 min at 20 °C, followed by addition of the labeled probe and incubation for a further 10 min at 20 °C. In all cases, results were developed and digitalized with a Fuji phosphorimager (GE Healthcare).

RNA Isolation and Real Time PCR Quantifications—RNA was extracted from early log-phase cultures of *M. tuberculosis* as described previously (55). A mid-log culture of indicated strains grown in 7H9 medium was diluted 100-fold into the same medium and grown to an A_{600} of ~0.3. cDNA synthesis and PCRs were carried out using a one-step RT-PCR kit (Superscript III platinum-SYBR Green; Invitrogen) with appropriate primer pairs (200 nM) as described previously (55). Expression of *espR*, *espB,* and *espACD* was quantified after normalization of RNA levels to the expression of *M. tuberculosis gapdh* mRNA, which served as the endogenous control; *gapdh* gene-specific primers have been described previously (55). Average fold changes and standard deviations were calculated using the $\Delta\Delta C_T$ method (59). Control reactions with platinum *Taq*DNA polymerase (Invitrogen) confirmed the absence of genomic DNA in RNA preparations.

Immunoblotting—For Western blot analyses, the indicated amounts of total protein from culture filtrates or cell lysates were resolved by SDS-PAGE and transferred to PVDF membranes (Millipore). To identify specific proteins, the membranes were probed with primary antibody as appropriate and visualized by using a horseradish peroxidase-conjugated secondary antibody. Culture filtrates and cell lysates were collected from indicated *M. tuberculosis* cultures as described above. αGroEL2 was used as a lysis control of culture filtrates to confirm that the secretion differences described here were not due to bacterial cytolysis. Anti-PhoP antibody was elicited in rabbit and affinity-purified using full-length purified recombinant PhoP (Abexome Biosciences). EspA-reactive serum was a kind gift from Dr. Sarah Fortune. Anti-ESAT-6 was from Santa Cruz Biotechnology; antibodies against EspR and RpoB were obtained from Abcam; and anti-His antibody was from GE Healthcare.

ChIP Assays—ChIP experiments in actively growing cultures of WT and mutant *M. tuberculosis* strains involved immunoprecipitation (IP) using anti-PhoP (Abexome Biosciences) or anti-EspR antibody (Abcam) and were carried out essentially as described previously (60). Briefly, DNA-protein complexes in growing cells were cross-linked for 20 min by 1% formaldehyde. Cross-linking was quenched by the addition of 0.3 M glycine. Typically, 20-ml cultures were collected by centrifugation, washed at least twice with 10 ml of IP (50 mM Tris-HCl (pH 7.5), 150 mM NaCl, 1 mM EDTA (pH 8.0), 1 mM phenylmethylsulfonyl fluoride, 5% glycerol, 1% Triton X-100) buffer to remove excess formaldehyde. Cells were resuspended in 0.5 ml of IP buffer and disrupted by bead-beating using 100 μm of zirconia

glass beads. Cell lysates were then diluted with 0.2 ml of IP buffer and cellular DNA was sonicated (five times for 20 s with a cooling interval of 30 s between each pulse) to an average size of ≈500 bp. After removing the cell debris, typically 0.2 ml of clear supernatant was used as total lysate for each IP experiment. *In vivo* recruitment of PhoP and EspR at the espAup was examined by ChIP-qPCR to detect promoter regions of interest. qPCR was performed using PAGE-purified primer pairs (Sigma) (supplemental Table S2) that spanned the *espACD* promoter region(s) of interest. PCR was performed by using appropriate dilutions of IP DNA in a reaction buffer containing SYBR Green mix, specific primers (0.4 μM), and 1 unit of Platinum *Taq*DNA polymerase (Invitrogen). Finally, region-specific recruitment was assessed by enrichment of PCR signal from the anti-PhoP or anti-EspR IP, and the results were normalized against PCR signal from mock sample (no antibody sample as a negative control) to determine fold enrichment of the PCR signal. Typically, 40 cycles of amplification were carried out using a real time PCR detection system (Eppendorf) with serially diluted DNA samples (mock, IP-treated, and total input). The specificity of PCR enrichment was verified by performing ChIP-qPCR of anti-EspR IP samples from the WT and mutant *M. tuberculosis* strains using 16S rRNA gene-specific primers as described previously (55). In all cases, ChIP experiments were repeated three times, and melting curve analysis confirmed amplification of a single product.

Macrophage Infection and Confocal Immunofluorescence Microscopy—0.25×10^6 RAW264.7 murine macrophages were seeded onto #1 thickness 18-mm diameter glass coverslips in a 12-well plate. At 40% confluency (0.5 million cells) macrophages were independently infected with WT *M. tuberculosis*-H37Rv and indicated mutant strains at a multiplicity of infection of 1:5 for 3 h at 37 °C in 5% CO_2. After infection, extracellular bacteria were removed by washing three times with pre-warmed phosphate-buffered saline (PBS). The cells were stained with 300 nM LysoTracker Red DND 99 (Invitrogen) and incubated in the CO_2 incubator for 3 h. The cells were fixed with 4% paraformaldehyde in PBS for 10 min. For visualization of *M. tuberculosis* strains, a fluorescent staining kit for mycobacteria (Sigma) was used. Briefly, the cells were stained with phenolic auramine solution (which selectively binds to mycolic acid) for 30 s followed by washing with PBS. The excess of auramine stain was removed by acid alcohol solution. The cells were washed three times with PBS, and the coverslips were mounted in Slow Fade-Anti-Fade (Invitrogen) and analyzed using a laser scanning confocal microscope (Nikon, A1R) equipped with argon (488 nm excitation line; 510 nm emission detection) and LD (561 nm excitation line; 594 nm emission detection) laser lines. Digital images were acquired and processed with image-processing software NIS elements (Nikon).The laser and the detector settings were optimized using macrophage cells infected with the WT bacteria, and the same standard set of intensity thresholds was applied to all images. The percentage of *M. tuberculosis* co-localized with LysoTracker was determined by analyzing more than 100 bacteria per sample from at least five random fields. The experiments were repeated at least five times.

Co-immunoprecipitation—For this purpose, WT *M. tuberculosis* H37Rv cell lysates containing ~1–1.5 mg of total protein were incubated with 50 μg of anti-PhoP antibody at 4 °C overnight. Next, ~20 μl of protein A/G-agarose beads (Thermo Scientific) were added to the samples, and incubation was further continued for 2 h at 4 °C. To study *in vitro* interactions between PhoP and EspR in *E. coli*, the *espR* ORF was cloned in-frame with the N-terminal His_6 tag of the first multiple cloning site of pRSF-Duet-1 vector (Table 1) between BamHI and HindIII sites. The *phoP* encoding ORF was cloned with the C-terminal S-tag of the second multiple cloning site of the same vector between NdeI and XhoI sites. The resultant construct was transformed in *E. coli* BL21(DE3), and protein expression was induced by addition of 0.4 mM isopropyl 1-thio-β-D-galactopyranoside at 18 °C with cells growing overnight. Next, cell extracts containing ~600 μg of total protein were immunoprecipitated using ~50 μg of anti-PhoP antibody as described above. Finally, the beads were collected by centrifugation and washed with 1× Tris-NaCl 3–5 times. In both cases, the protein samples were eluted by incubating the beads at 100 °C for 5 min in the presence of 50 μl of 2× SDS-PAGE buffer. Samples were analyzed by SDS-PAGE and visualized by Western blotting using anti-EspR antibody.

M-PFC Assays—This assay relies on the principle that two interacting mycobacterial proteins independently fused to the domains of murine dihydrofolate reductase if co-expressed in mycobacteria reconstitute functionally active murine dihydrofolate reductase enzyme, conferring bacterial resistance to trimethoprim (48). *M. tuberculosis phoP* and *phoR* genes were cloned in integrative vector pUAB400 (Kan^r) and episomal vector pUAB300 (Hyg^r), respectively (Table 1), and expressed in *M. smegmatis* as described previously (55); *espR* was cloned in episomal plasmid pUAB300 (Hyg^r) between BamHI/HindIII sites using primer pair mEspRFP/mEspRRP. The construct was verified by DNA sequencing.

Author Contributions—D. S. conceived and coordinated the study and wrote the paper. R. G. and V. A. K. designed, performed, and analyzed the experiments shown in Figs. 1, 3, and 4. V. A. K., N. S., and A. K. designed, performed, and analyzed the experiments shown in Fig. 2. R. B., V. A. K., R. R. S., and R. G. designed, performed, and analyzed the experiments shown in Fig. 5. All authors reviewed the results and approved the final version of the manuscript.

Acknowledgments—We thank Drs. G. Marcela Rodriguez and Issar Smith (Public Health Research Institute, Rutgers New Jersey Medical School) for ΔphoP, complemented ΔphoP strains of M. tuberculosis, and pSM128; Adrie Steyn (University of Alabama) for pUAB300/pUAB400 plasmids; Sarah Fortune (Harvard School of Public Health) for anti-EspA antisera; and Sabine Ehrt (Weil Medical College of Cornell University) for pME1mL1 expression vector. We are grateful to Dr. Issar Smith for critically reading the manuscript. We thank Renu Sharma for technical assistance and for help with the preparation of the manuscript.

References

1. Bitter, W., Houben, E. N., Bottai, D., Brodin, P., Brown, E. J., Cox, J. S., Derbyshire, K., Fortune, S. M., Gao, L. Y., Liu, J., Gey van Pittius, N. C., Pym, A. S., Rubin, E. J., Sherman, D. R., Cole, S. T., and Brosch, R. (2009)

Systematic genetic nomenclature for type VII secretion systems. *PLoS Pathog.* **5,** e1000507
2. Guinn, K. M., Hickey, M. J., Mathur, S. K., Zakel, K. L., Grotzke, J. E., Lewinsohn, D. M., Smith, S., and Sherman, D. R. (2004) Individual RD1-region genes are required for export of ESAT-6/CFP-10 and for virulence of *Mycobacterium tuberculosis*. *Mol. Microbiol.* **51,** 359–370
3. Hsu, T., Hingley-Wilson, S. M., Chen, B., Chen, M., Dai, A. Z., Morin, P. M., Marks, C. B., Padiyar, J., Goulding, C., Gingery, M., Eisenberg, D., Russell, R. G., Derrick, S. C., Collins, F. M., Morris, S. L., *et al.* (2003) The primary mechanism of attenuation of bacillus Calmette-Guerin is a loss of secreted lytic function required for invasion of lung interstitial tissue. *Proc. Natl. Acad. Sci. U.S.A.* **100,** 12420–12425
4. Simeone, R., Bottai, D., and Brosch, R. (2009) ESX/type VII secretion systems and their role in host-pathogen interaction. *Curr. Opin. Microbiol.* **12,** 4–10
5. Stanley, S. A., Raghavan, S., Hwang, W. W., and Cox, J. S. (2003) Acute infection and macrophage subversion by *Mycobacterium tuberculosis* require a specialized secretion system. *Proc. Natl. Acad. Sci. U.S.A.* **100,** 13001–13006
6. Bentley, S. D., Comas, I., Bryant, J. M., Walker, D., Smith, N. H., Harris, S. R., Thurston, S., Gagneux, S., Wood, J., Antonio, M., Quail, M. A., Gehre, F., Adegbola, R. A., Parkhill, J., and de Jong, B. C. (2012) The genome of *Mycobacterium africanum* West African 2 reveals a lineage-specific locus and genome erosion common to the *Mycobacterium tuberculosis* complex. *PLoS Negl. Trop. Dis.* **6,** e1552
7. Cole, S. T., Eiglmeier, K., Parkhill, J., James, K. D., Thomson, N. R., Wheeler, P. R., Honoré, N., Garnier, T., Churcher, C., Harris, D., Mungall, K., Basham, D., Brown, D., Chillingworth, T., Connor, R., *et al.* (2001) Massive gene decay in the leprosy *Bacillus*. *Nature* **409,** 1007–1011
8. Garnier, T., Eiglmeier, K., Camus, J. C., Medina, N., Mansoor, H., Pryor, M., Duthoy, S., Grondin, S., Lacroix, C., Monsempe, C., Simon, S., Harris, B., Atkin, R., Doggett, J., Mayes, R., *et al.* (2003) The complete genome sequence of *Mycobacterium bovis*. *Proc. Natl. Acad. Sci. U.S.A.* **100,** 7877–7882
9. Stinear, T. P., Seemann, T., Harrison, P. F., Jenkin, G. A., Davies, J. K., Johnson, P. D., Abdellah, Z., Arrowsmith, C., Chillingworth, T., Churcher, C., Clarke, K., Cronin, A., Davis, P., Goodhead, I., Holroyd, N., *et al.* (2008) Insights from the complete genome sequence of *Mycobacterium marinum* on the evolution of *Mycobacterium tuberculosis*. *Genome Res.* **18,** 729–741
10. Brodin, P., de Jonge, M. I., Majlessi, L., Leclerc, C., Nilges, M., Cole, S. T., and Brosch, R. (2005) Functional analysis of early secreted antigenic target-6, the dominant T-cell antigen of *Mycobacterium tuberculosis*, reveals key residues involved in secretion, complex formation, virulence, and immunogenicity. *J. Biol. Chem.* **280,** 33953–33959
11. Brodin, P., Majlessi, L., Marsollier, L., de Jonge, M. I., Bottai, D., Demangel, C., Hinds, J., Neyrolles, O., Butcher, P. D., Leclerc, C., Cole, S. T., and Brosch, R. (2006) Dissection of ESAT-6 system 1 of *Mycobacterium tuberculosis* and impact on immunogenicity and virulence. *Infect. Immun.* **74,** 88–98
12. Derrick, S. C., and Morris, S. L. (2007) The ESAT6 protein of *Mycobacterium tuberculosis* induces apoptosis of macrophages by activating caspase expression. *Cell. Microbiol.* **9,** 1547–1555
13. Fortune, S. M., Jaeger, A., Sarracino, D. A., Chase, M. R., Sassetti, C. M., Sherman, D. R., Bloom, B. R., and Rubin, E. J. (2005) Mutually dependent secretion of proteins required for mycobacterial virulence. *Proc. Natl. Acad. Sci. U.S.A.* **102,** 10676–10681
14. Houben, D., Demangel, C., van Ingen, J., Perez, J., Baldeón, L., Abdallah, A. M., Caleechurn, L., Bottai, D., van Zon, M., de Punder, K., van der Laan, T., Kant, A., Bossers-de Vries, R., Willemsen, P., Bitter, W., *et al.* (2012) ESX-1-mediated translocation to the cytosol controls virulence of mycobacteria. *Cell. Microbiol.* **14,** 1287–1298
15. Lewis, K. N., Liao, R., Guinn, K. M., Hickey, M. J., Smith, S., Behr, M. A., and Sherman, D. R. (2003) Deletion of RD1 from *Mycobacterium tuberculosis* mimics bacille Calmette-Guerin attenuation. *J. Infect. Dis.* **187,** 117–123
16. Majlessi, L., Brodin, P., Brosch, R., Rojas, M. J., Khun, H., Huerre, M., Cole, S. T., and Leclerc, C. (2005) Influence of ESAT-6 secretion system 1 (RD1) of *Mycobacterium tuberculosis* on the interaction between mycobacteria and the host immune system. *J. Immunol.* **174,** 3570–3579
17. Pym, A. S., Brodin, P., Brosch, R., Huerre, M., and Cole, S. T. (2002) Loss of RD1 contributed to the attenuation of the live tuberculosis vaccines *Mycobacterium bovis* BCG and *Mycobacterium microti*. *Mol. Microbiol.* **46,** 709–717
18. Stanley, S. A., Johndrow, J. E., Manzanillo, P., and Cox, J. S. (2007) The type I IFN response to infection with *Mycobacterium tuberculosis* requires ESX-1-mediated secretion and contributes to pathogenesis. *J. Immunol.* **178,** 3143–3152
19. Tan, T., Lee, W. L., Alexander, D. C., Grinstein, S., and Liu, J. (2006) The ESAT-6/CFP-10 secretion system of *Mycobacterium marinum* modulates phagosome maturation. *Cell. Microbiol.* **8,** 1417–1429
20. Pym, A. S., Brodin, P., Majlessi, L., Brosch, R., Demangel, C., Williams, A., Griffiths, K. E., Marchal, G., Leclerc, C., and Cole, S. T. (2003) Recombinant BCG exporting ESAT-6 confers enhanced protection against tuberculosis. *Nat. Med.* **9,** 533–539
21. MacGurn, J. A., Raghavan, S., Stanley, S. A., and Cox, J. S. (2005) A non-RD1 gene cluster is required for Snm secretion in *Mycobacterium tuberculosis*. *Mol. Microbiol.* **57,** 1653–1663
22. Garces, A., Atmakuri, K., Chase, M. R., Woodworth, J. S., Krastins, B., Rothchild, A. C., Ramsdell, T. L., Lopez, M. F., Behar, S. M., Sarracino, D. A., and Fortune, S. M. (2010) EspA acts as a critical mediator of ESX1-dependent virulence in *Mycobacterium tuberculosis* by affecting bacterial cell wall integrity. *PLoS Pathog.* **6,** e1000957
23. Frigui, W., Bottai, D., Majlessi, L., Monot, M., Josselin, E., Brodin, P., Garnier, T., Gicquel, B., Martin, C., Leclerc, C., Cole, S. T., and Brosch, R. (2008) Control of *M. tuberculosis* ESAT-6 secretion and specific T cell recognition by PhoP. *PLoS Pathog.* **4,** e33
24. Ryndak, M., Wang, S., and Smith, I. (2008) PhoP, a key player in *Mycobacterium tuberculosis* virulence. *Trends Microbiol.* **16,** 528–534
25. Gonzalo-Asensio, J., Mostowy, S., Harders-Westerveen, J., Huygen, K., Hernández-Pando, R., Thole, J., Behr, M., Gicquel, B., and Martín, C. (2008) PhoP: a missing piece in the intricate puzzle of *Mycobacterium tuberculosis* virulence. *PloS one* **3,** e3496
26. Lee, J. S., Krause, R., Schreiber, J., Mollenkopf, H. J., Kowall, J., Stein, R., Jeon, B. Y., Kwak, J. Y., Song, M. K., Patron, J. P., Jorg, S., Roh, K., Cho, S. N., and Kaufmann, S. H. (2008) Mutation in the transcriptional regulator PhoP contributes to avirulence of *Mycobacterium tuberculosis* H37Ra strain. *Cell Host Microbe* **3,** 97–103
27. Walters, S. B., Dubnau, E., Kolesnikova, I., Laval, F., Daffe, M., and Smith, I. (2006) The *Mycobacterium tuberculosis* PhoPR two-component system regulates genes essential for virulence and complex lipid biosynthesis. *Mol. Microbiol.* **60,** 312–330
28. Kahramanoglou, C., Cortes, T., Matange, N., Hunt, D. M., Visweswariah, S. S., Young, D. B., and Buxton, R. S. (2014) Genomic mapping of cAMP receptor protein (CRP Mt) in *Mycobacterium tuberculosis*: relation to transcriptional start sites and the role of CRPMt as a transcription factor. *Nucleic Acids Res.* **42,** 8320–8329
29. Raghavan, S., Manzanillo, P., Chan, K., Dovey, C., and Cox, J. S. (2008) Secreted transcription factor controls *Mycobacterium tuberculosis* virulence. *Nature* **454,** 717–721
30. Gordon, B. R., Li, Y., Wang, L., Sintsova, A., van Bakel, H., Tian, S., Navarre, W. W., Xia, B., and Liu, J. (2010) Lsr2 is a nucleoid-associated protein that targets AT-rich sequences and virulence genes in *Mycobacterium tuberculosis*. *Proc. Natl. Acad. Sci. U.S.A.* **107,** 5154–5159
31. Pang, X., Samten, B., Cao, G., Wang, X., Tvinnereim, A. R., Chen, X. L., and Howard, S. T. (2013) MprAB regulates the espA operon in *Mycobacterium tuberculosis* and modulates ESX-1 function and host cytokine response. *J. Bacteriol.* **195,** 66–75
32. Minch, K. J., Rustad, T. R., Peterson, E. J., Winkler, J., Reiss, D. J., Ma, S., Hickey, M., Brabant, W., Morrison, B., Turkarslan, S., Mawhinney, C., Galagan, J. E., Price, N. D., Baliga, N. S., and Sherman, D. R. (2015) The DNA-binding network of *Mycobacterium tuberculosis*. *Nat. Commun.* **6,** 5829
33. Broset, E., Martín, C., and Gonzalo-Asensio, J. (2015) Evolutionary landscape of the *Mycobacterium tuberculosis* complex from the viewpoint of PhoPR: implications for virulence regulation and application to vaccine development. *MBio* **6,** e01289–15

34. Majlessi, L., Prados-Rosales, R., Casadevall, A., and Brosch, R. (2015) Release of mycobacterial antigens. *Immunol. Rev.* **264,** 25–45
35. Solans, L., Aguiló, N., Samper, S., Pawlik, A., Frigui, W., Martín, C., Brosch, R., and Gonzalo-Asensio, J. (2014) A specific polymorphism in *Mycobacterium tuberculosis* H37Rv causes differential ESAT-6 expression and identifies WhiB6 as a novel ESX-1 component. *Infect. Immun.* **82,** 3446–3456
36. Gonzalo-Asensio, J., Malaga, W., Pawlik, A., Astarie-Dequeker, C., Passemar, C., Moreau, F., Laval, F., Daffé, M., Martin, C., Brosch, R., and Guilhot, C. (2014) Evolutionary history of tuberculosis shaped by conserved mutations in the PhoPR virulence regulator. *Proc. Natl. Acad. Sci. U.S.A.* **111,** 11491–11496
37. He, X., and Wang, S. (2014) DNA consensus sequence motif for binding response regulator PhoP, a virulence regulator of *Mycobacterium tuberculosis*. *Biochemistry* **53,** 8008–8020
38. Rosenberg, O. S., Dovey, C., Tempesta, M., Robbins, R. A., Finer-Moore, J. S., Stroud, R. M., and Cox, J. S. (2011) EspR, a key regulator of *Mycobacterium tuberculosis* virulence, adopts a unique dimeric structure among helix-turn-helix proteins. *Proc. Natl. Acad. Sci. U.S.A.* **108,** 13450–13455
39. Cao, G., Howard, S. T., Zhang, P., Wang, X., Chen, X. L., Samten, B., and Pang, X. (2015) EspR, a regulator of the ESX-1 secretion system in *Mycobacterium tuberculosis*, is directly regulated by the two-component systems MprAB and PhoPR. *Microbiology* **161,** 477–489
40. Blasco, B., Stenta, M., Alonso-Sarduy, L., Dietler, G., Peraro, M. D., Cole, S. T., and Pojer, F. (2011) Atypical DNA recognition mechanism used by the EspR virulence regulator of *Mycobacterium tuberculosis*. *Mol. Microbiol.* **82,** 251–264
41. Solans, L., Gonzalo-Asensio, J., Sala, C., Benjak, A., Uplekar, S., Rougemont, J., Guilhot, C., Malaga, W., Martín, C., and Cole, S. T. (2014) The PhoP-dependent ncRNA Mcr7 modulates the TAT secretion system in *Mycobacterium tuberculosis*. *PLoS Pathog.* **10,** e1004183
42. Blasco, B., Chen, J. M., Hartkoorn, R., Sala, C., Uplekar, S., Rougemont, J., Pojer, F., and Cole, S. T. (2012) Virulence regulator EspR of *Mycobacterium tuberculosis* is a nucleoid-associated protein. *PLoS Pathog.* **8,** e1002621
43. Hunt, D. M., Sweeney, N. P., Mori, L., Whalan, R. H., Comas, I., Norman, L., Cortes, T., Arnvig, K. B., Davis, E. O., Stapleton, M. R., Green, J., and Buxton, R. S. (2012) Long-range transcriptional control of an operon necessary for virulence-critical ESX-1 secretion in *Mycobacterium tuberculosis*. *J. Bacteriol.* **194,** 2307–2320
44. Gordon, S. V., Brosch, R., Billault, A., Garnier, T., Eiglmeier, K., and Cole, S. T. (1999) Identification of variable regions in the genomes of tubercle bacilli using bacterial artificial chromosome arrays. *Mol. Microbiol.* **32,** 643–655
45. Xu, J., Laine, O., Masciocchi, M., Manoranjan, J., Smith, J., Du, S. J., Edwards, N., Zhu, X., Fenselau, C., and Gao, L. Y. (2007) A unique *Mycobacterium* ESX-1 protein co-secretes with CFP-10/ESAT-6 and is necessary for inhibiting phagosome maturation. *Mol. Microbiol.* **66,** 787–800
46. Romagnoli, A., Etna, M. P., Giacomini, E., Pardini, M., Remoli, M. E., Corazzari, M., Falasca, L., Goletti, D., Gafa, V., Simeone, R., Delogu, G., Piacentini, M., Brosch, R., Fimia, G. M., and Coccia, E. M. (2012) ESX-1 dependent impairment of autophagic flux by *Mycobacterium tuberculosis* in human dendritic cells. *Autophagy* **8,** 1357–1370
47. Chesne-Seck, M. L., Barilone, N., Boudou, F., Gonzalo Asensio, J., Kolattukudy, P. E., Martín, C., Cole, S. T., Gicquel, B., Gopaul, D. N., and Jackson, M. (2008) A point mutation in the two-component regulator PhoP-PhoR accounts for the absence of polyketide-derived acyltrehaloses but not that of phthiocerol dimycocerosates in *Mycobacterium tuberculosis* H37Ra. *J. Bacteriol.* **190,** 1329–1334
48. Singh, A., Mai, D., Kumar, A., and Steyn, A. J. (2006) Dissecting virulence pathways of *Mycobacterium tuberculosis* through protein-protein association. *Proc. Natl. Acad. Sci. U.S.A.* **103,** 11346–11351
49. Coros, A., Callahan, B., Battaglioli, E., and Derbyshire, K. M. (2008) The specialized secretory apparatus ESX-1 is essential for DNA transfer in *Mycobacterium smegmatis*. *Mol. Microbiol.* **69,** 794–808
50. Flint, J. L., Kowalski, J. C., Karnati, P. K., and Derbyshire, K. M. (2004) The RD1 virulence locus of *Mycobacterium tuberculosis* regulates DNA transfer in *Mycobacterium smegmatis*. *Proc. Natl. Acad. Sci. U.S.A.* **101,** 12598–12603
51. He, X., Wang, L., and Wang, S. (2016) Structural basis of DNA sequence recognition by the response regulator PhoP in *Mycobacterium tuberculosis*. *Sci. Rep.* **6,** 24442
52. Snapper, S. B., Melton, R. E., Mustafa, S., Kieser, T., and Jacobs, W. R., Jr. (1990) Isolation and characterization of efficient plasmid transformation mutants of *Mycobacterium smegmatis*. *Mol. Microbiol.* **4,** 1911–1919
53. Jacobs, W. R., Jr, Kalpana, G. V., Cirillo, J. D., Pascopella, L., Snapper, S. B., Udani, R. A., Jones, W., Barletta, R. G., and Bloom, B. R. (1991) Genetic systems for mycobacteria. *Methods Enzymol.* **204,** 537–555
54. Goyal, R., Das, A. K., Singh, R., Singh, P. K., Korpole, S., and Sarkar, D. (2011) Phosphorylation of PhoP protein plays direct regulatory role in lipid biosynthesis of *Mycobacterium tuberculosis*. *J. Biol. Chem.* **286,** 45197–45208
55. Singh, R., Anil Kumar, V., Das, A. K., Bansal, R., and Sarkar, D. (2014) A transcriptional co-repressor regulatory circuit controlling the heat-shock response of *Mycobacterium tuberculosis*. *Mol. Microbiol.* **94,** 450–465
56. De Smet, K. A., Kempsell, K. E., Gallagher, A., Duncan, K., and Young, D. B. (1999) Alteration of a single amino acid residue reverses fosfomycin resistance of recombinant MurA from *Mycobacterium tuberculosis*. *Microbiology* **145,** 3177–3184
57. Dussurget, O., Timm, J., Gomez, M., Gold, B., Yu, S., Sabol, S. Z., Holmes, R. K., Jacobs, W. R., Jr., and Smith, I. (1999) Transcriptional control of the iron-responsive fxbA gene by the mycobacterial regulator IdeR. *J. Bacteriol.* **181,** 3402–3408
58. Gupta, S., Pathak, A., Sinha, A., and Sarkar, D. (2009) *Mycobacterium tuberculosis* PhoP recognizes two adjacent direct-repeat sequences to form head-to-head dimers. *J. Bacteriol.* **191,** 7466–7476
59. Schmittgen, T. D., and Livak, K. J. (2008) Analyzing real-time PCR data by the comparative $C(T)$ method. *Nat. Protoc.* **3,** 1101–1108
60. Fol, M., Chauhan, A., Nair, N. K., Maloney, E., Moomey, M., Jagannath, C., Madiraju, M. V., and Rajagopalan, M. (2006) Modulation of *Mycobacterium tuberculosis* proliferation by MtrA, an essential two-component response regulator. *Mol. Microbiol.* **60,** 643–657
61. Ehrt, S., Guo, X. V., Hickey, C. M., Ryou, M., Monteleone, M., Riley, L. W., and Schnappinger, D. (2005) Controlling gene expression in mycobacteria with anhydrotetracycline and Tet repressor. *Nucleic Acids Res.* **33,** e21